Indian Journal of Engineering & Materials Sciences
Vol. 29, August 2022, pp. 493-501
DOI: 10.56042/ijems.v29i4.46396

Determination of thermal properties of ternary Al-La-Ni cast alloy

Emin Çadırlı[a*], & Erkan Üstün[b]

[a]Niğde Ömer Halisdemir University, Faculty of Arts and Sciences, Department of Physics, 51240 Niğde, Turkey

[b]Niğde Ömer Halisdemir University, Institute of Science, 51240 Niğde, Turkey

Received: 14 February 2021; Accepted: 1 September 2021

In current work, thermal conductivity, enthalpy of fusion, specific heat, and thermal diffusivity of the Al-8.8La-1.2Ni cast alloy has been investigated. Chemical element analysis of the studied alloy was determined with X-Ray Fluorescence Spectrometer (XRF) and SEM microscopy with Energy Dispersive X-Ray Spectroscopy (EDS). Thermal conductivity of as-cast Al-8.8La-1.2Ni alloy was measured using comparison cut bar method in the temperature range of 308–773 K. Thermal conductivity values decreased gradually in the studied alloy with the increase of temperature. The thermal temperature coefficient was calculated from the thermal conductivity-temperature graph. The heat flow-temperature curve was obtained by performing Differential Scanning Calorimetry (DSC) analysis. Enthalpy of fusion and specific heat values were also determined. Thermal diffusivity values were calculated as a function of temperature using the relevant equation. It was determined that the thermal diffusivity values increased with increasing temperature.

Keywords: Ternary alloys, Cut Bar Method, Heat Flow, Steady-State Measurement

1 Introduction

Along with durability in many engineering fields such as automotive, aircraft and aerospace engineering, the main trend is to improve engine efficiency and fuel economy. Therefore, it is very important for these sectors to produce new materials with improved thermal and mechanical properties. Al-based alloys with superior special strength, high plasticity, low and high temperatures have formed the main structural materials of such sectors[1-4].

In order to better understand the thermal behavior, three basic parameters that affect the thermal properties of materials can be mentioned;

These thermal parameters are thermal conductivity (λ), specific heat (C_p) and thermal diffusivity (α). These three parameters have very important effects on many thermal processes such as cold working, extrusion, and welding. While measuring the thermal conductivity of materials, there are methods used in different temperature ranges suitable for the type and size of the materials[5-19].

In this study, "the comparative cut bar process" was chosen for our alloy. This process is commonly used especially in scientific research and development studies. The positive and negative aspects of this test procedure have been discussed in some studies [20-22].

In this context, many researchers have done numerous works, especially in improvement of the thermal properties of metallic alloys (hot forging, cold working, chill casting, extrusion, heat treatment, hybrid alloying etc.)[19-27]. The thermal properties of the Al-8.8La-1.2Ni ternary alloy, which is known for its good glass-forming abilities through liquid state rapid quenching[28] and hydrogen storage capabilities in solid state[29], were preferred to study. These alloys are potential candidates for technological applications due to these aforementioned properties. Although the Al-8.8La-1.2Ni ternary alloy has a commercially important place, there are hardly any studies in the literature describing some of the thermal properties of its alloy depending on the temperature. For Al-based alloy systems, some studies have been carried out showing the variation of thermal conductivity depending on ambient conditions or temperature in a narrow temperature range[23-27].

Pariona *et al.*[26] investigated the thermal conductivity of Al-1Ni alloy in the narrow temperature range of 910-937 K under different heat treatment conditions. They reported that the thermal conductivity decreased from 202 to 82 $Wm^{-1}K^{-1}$ with increasing temperature.

It is known that the growth rate of solidified materials has a significant effect on the microstructure and mechanical properties. In this context, to

*Corresponding author (E-mail: ecadirli@gmail.com)

investigate whether the growth rate has a possible effect on thermal conductivity, Al-32.5Cu-1Ni alloy was directionally solidified at constant G and different V by Bayram *et al.*[27] using Bridgman type furnace. Then, the thermal conductivity of these samples for each growth rate at room temperature was measured using the longitudinal heat flow apparatus technique. They found that the thermal conductivity decreased from 235.64 to 195.92 W/Km with the increase in the growth rate. Determining the thermal properties of the alloy we have chosen by examining our sample, which is in the as cast without mechanical or thermal treatment, in a wide temperature range (~308-773 K) makes us different from other studies. Therefore, the aim of this study is to determine the λ, α and C_p of the studied alloy the temperature-dependent in a broad temperature range. In this context, studies were carried out in three stages. Firstly, the thermal conductivity change of Al-8.8La-1.2Ni samples were measured using the "comparative cut bar method" in the temperature range of ~ 308–773 K. Secondly, the heat flow-temperature curve was obtained using the DSC technique and the fusion enthalpy (ΔH) and Cp values were determined from this curve. In the third stage, these thermal data obtained were used in the related equation and α values were calculated as a function of T.

2 Materials and Methods

2.1. Sample preparation

Al, La and Ni metals with 99.99% purity were used in the production of the Al-8.8La-1.2Ni alloy (compositions of alloys attributed in this study are given as weight percent). After adjusting the Al, La and Ni metal amounts, they were inserted in a graphite crucible and melted in a vacuum melting furnace. Graphite crucible was preferred in our experiment system because it λ is better than alumina and it can be processed more easily on a lathe. After manual stirring of the melt at certain time intervals to obtain a sufficiently homogeneous melt (approximately 50-60 K above the melting point of the alloy), the molten alloy was poured into cylindrical alumina crucibles (4x7x200 mm) pre-placed in the casting furnace (Fig. 1) by means of a graphite funnel. Later, alumina crucibles filled with the molten alloy were mixed with a thin alumina rod to prevent possible air bubbles. Details of the sample production process are given in a previous study by the authors[30].

2.2. Measurement of thermal conductivity

In "the comparative cut bar process", a test sample of unknown thermal conductivity (Al-8.8La-1.2 Ni casting sample) is sandwiched between two reference materials (pure Al) materials with known thermal conductivity. Thermal grease is used to ensure good contact and minimize interfacial resistances.

Fourier conduction equation;

$$Q = -\lambda A \frac{dT}{dx} \quad \text{... (1)}$$

where, Q is power, λ is the thermal conductivity, A is the circular cross-sectional area of the test sample and dT/dx is the temperature gradient of the region where the temperature is measured.

A schematic diagram of the "comparative cut bar process" is shown in Fig. 2. As shown in Fig. 2b, a test sample of unknown thermal conductivity (λ_s) was placed between two reference samples (pure Al) with well-known thermal conductivity (λ_r). Temperature measurements measured three times from the red dots at steady state (for statistical reliability). The heat flux through the reference and test samples in the sandwiched state can be calculated from the expression:

$$\frac{Q}{A} = -\lambda_s \frac{\Delta T_{34}}{\Delta X_{34}} = \frac{\lambda_r}{2}\left(\frac{\Delta T_{12}}{\Delta X_{12}} + \frac{\Delta T_{56}}{\Delta X_{56}}\right) \quad \text{... (2)}$$

The axial heat flow furnace (as seen in Fig. 2) consists of three main parts. These are hot zone, cold zone and driver system. The drive system is located at the bottom of the axial heat flow furnace and ensures that the samples are in the proper position. In order to obtain a stable longitudinal heat flow, the samples in contact are effectively cooled from the bottom by the water cooling system. A refrigerating water circulation system is used to ensure effective cooling of the sample from the bottom, thereby achieving sufficiently large temperature gradients (Fig. 2 (b)). Lateral heat losses are reduced as much as possible by using suitable insulation materials.

As can be seen in Fig. 2(a), the experimental measurement system was fed with argon gas at reasonable flow rates to avoid any oxidation Such measurements[16] are also not recommended as vacuum can increase their thermal contact resistance. The radial heat loss of the samples can sometimes be more important than the longitudinal contact resistance of the samples. In particular, these should be taken into

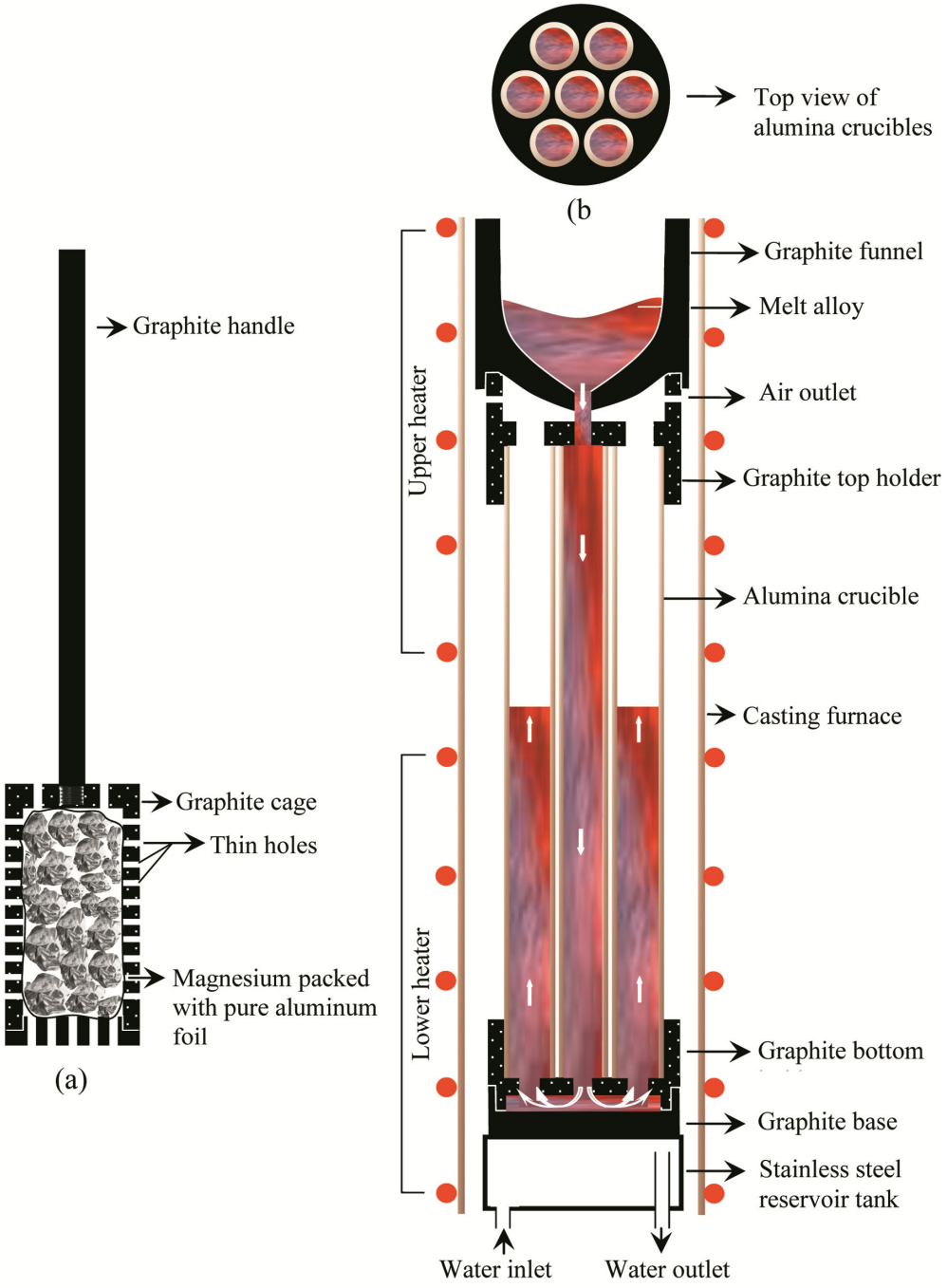

Fig. 1 — (a) Graphite cage and holder, (b) Top view of alumina crucibles, and (c) the casting furnace.

account. Therefore, argon with lower conductivity was chosen in this experimental process. The axial heat flow furnace was heated in 50 K steps from RT to approximately 800 K. A high precision temperature controller (±0.05K) was used to avoid temperature fluctuation as much as possible inside the axial heat flow furnace. For each temperature step to be measured, the samples were kept at the desired temperature for at least 120 minutes in a steady state condition. In the steady state condition, the temperatures of the test and reference samples (red dots, see Figure 2(b) were measured with a 0.5 mm diameter K-type thermocouple. A well-equipped computer was used to record all temperature data during the experiment. During these measurements, the experimental error was found to be approximately 5%.

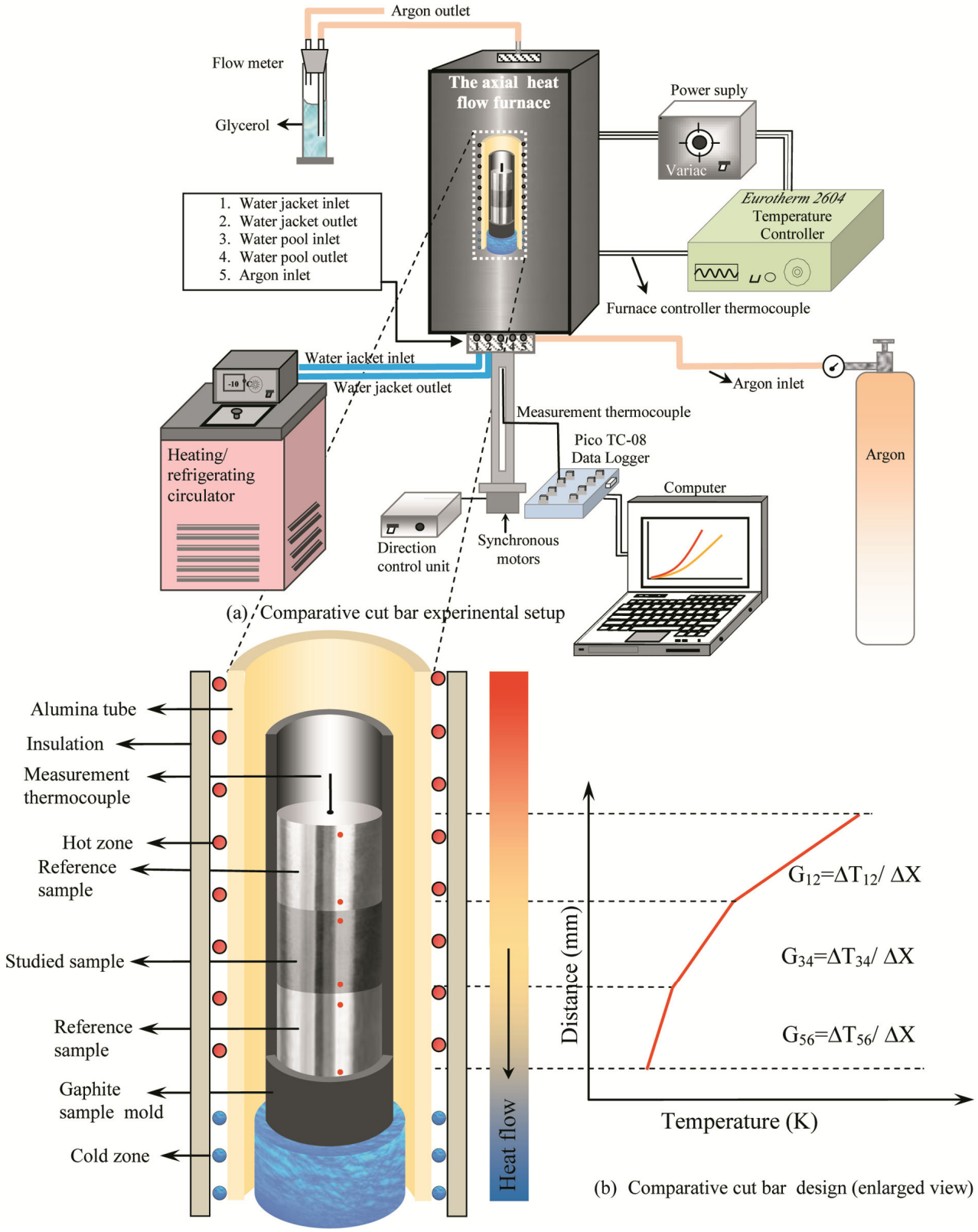

Fig. 2 — (a) Schematic view of the experimental design (b) Comparative cut bar design for thermal conductivity measurement (enlarged view).

The temperature dependence relation for λ of the solid phase of the material can be expressed as:

$$\lambda = \lambda_o\left[1 + \alpha_{TTC}\left(T - T_o\right)\right] \quad \text{... (3a)}$$

and the thermal temperature coefficient, $\alpha_{TTC,}$ is expressed as[10]

$$\alpha_{TTC} = \frac{\lambda - \lambda_o}{\lambda_o(T - T_o)} = \frac{1}{\lambda_o}\frac{\Delta K}{\Delta T} \quad \text{... (3b)}$$

where, λ_o is the thermal conductivity at the T_o (RT).

2.3. Determination of ΔH, Cp and thermal diffusivity

DSC analysis was done using Netzsch STA 449F3 Jupiter device and heat flow curve was obtained. The Cp value is determined using this curve and is expressed by the following equation.

$$mC_p\frac{dT}{dt} = \frac{dQ}{dt} \quad \text{... (4)}$$

The melting temperature was determined with an accuracy of ±0.2 K, and the enthalpy value was determined with an error of approximately 5%. Thermal diffusivity (α) is defined as how fast heat can transfer from hot region to cold region. α has a very effective role on the heat dissipation kinetics. The response of materials with high α to temperature changes is quite quickly. This situation indicates low thermal inertia.

The α value can be calculated with the Eq.5 given below.

$$\alpha = \frac{\lambda}{\rho C_p} \quad \text{... (5)}$$

where, ρ is the density (kg/m^3). Density, which varies with temperature, was calculated using eq.(6).

$$\rho(T) = \frac{\rho T_{RT}}{(1 - \alpha_T(T - T_{RT}))^3} \quad \text{... (6)}$$

where, α_T is the thermal expansion coefficient, and T_{RT} is the room temperature.

3 Results and Discussion

3.1. Determination of compositions

X-Ray Fluorescence (XRF) technique is used for long-term chemical analysis of alloys. This technique allows the quantitative identification of the elements present in alloy. In Table 1 gives the compositions obtained for the alloy examined by XRF using a Panalytical/Zetium model device. The composition amounts of Al, La, Ni, and other impurities (as seen in Table 1) were found to be 90.06, 8.62, 1.08, and 0.24 %, respectively. In addition, energy dispersive spectroscopy (EDS) / mapping analysis of the test sample (as-cast) have been performed (Fig. 3). As shown in the EDS spectrum (Fig. 3(b)), the composition values for Al, La and Ni were determined as 89.16, 9.64 and 1.21, respectively. These composition values largely agree with both the nominal composition values of the test sample and the composition values obtained from XRF analysis on the bulk sample. There is an almost homogeneous distribution in terms of components in the test sample, since no significant microsegregation occurs (Fig. 3(c-e)). The homogeneity of the test sample is one of the most important indicators showing that thermal conductivity measurements are reliable.

3.2 The temperature dependence of the thermal conductivity

The variation of the λ values of pure Al [31] and the studied alloy with temperature is shown in Fig. 4. In this figure, λ values decrease with increasing temperature. In Fig. 5, the changes in λ values of related pure metals, studied alloy and other Al-based alloys compiled from the literature with temperature are given collectively. While the λ values of pure Al[31], pure Ni[32], studied alloy and some Al alloys[23-27, 33-36] decrease with increasing T, the λ values of pure La [31] increase with increasing T. Figure 5 shows that the λ values of all the studied aluminum alloys in the literature are much lower than that of pure Al. The λ values decreasing with T for Al-8.8La-1.2Ni alloy are fairly below the line of λ variation with T for Al-6.1Zn-2.3Mg-1.9Cu[23], Al-5.6 Zn-2.5 Mg-1.6 Cu[24], pure Al[31], Al-1 Mg alloy[33], Al-5Zn[34], and Al-0.7Mg-0.4Si[35]. In addition, the λ values obtained for the studied alloy were slightly higher than those obtained for Al-3.25 Zn-1.9Mg-1.8Cu alloy[25], pure Ni[32], 7075/AlN Composite[36], and Al-5.5Zn-2.5Mg[37].

As shown in Fig. 5, the values of λ decreased from 240, 185 and 92 W/m K to 213, 143 and 60 W/m K with increasing T for the pure Al[31], Al-8.8La-1.2Ni and pure Ni[32], respectively. However, with increasing T, the λ value of pure La[31] has increased from 11.7 to

Table 1 — The chemical element analysis with XRF of the studied cast alloy

Element	La	Ni	Si	Fe	Na	other	Al
(Wt.%)	8.62	1.08	0.12	0.07	0.03	0.02	Balance

14.8. Considering the λ-T curves given for different Al-based alloys, we can make the following comments.

The total decrease in λ is approximately 23 % for studied alloy (Al-8.8La-1.2Ni). Smith[35] investigated thermal behaviour of the sintered Al-0.7Mg-0.4Si alloy and reported that λ decreased from 228 to 222 W/m K in the range of temperature 373-523 K.

Erol *et al.*[34] examined the variation of the λ of Al-5Zn alloy with increasing T. Using the radial heat

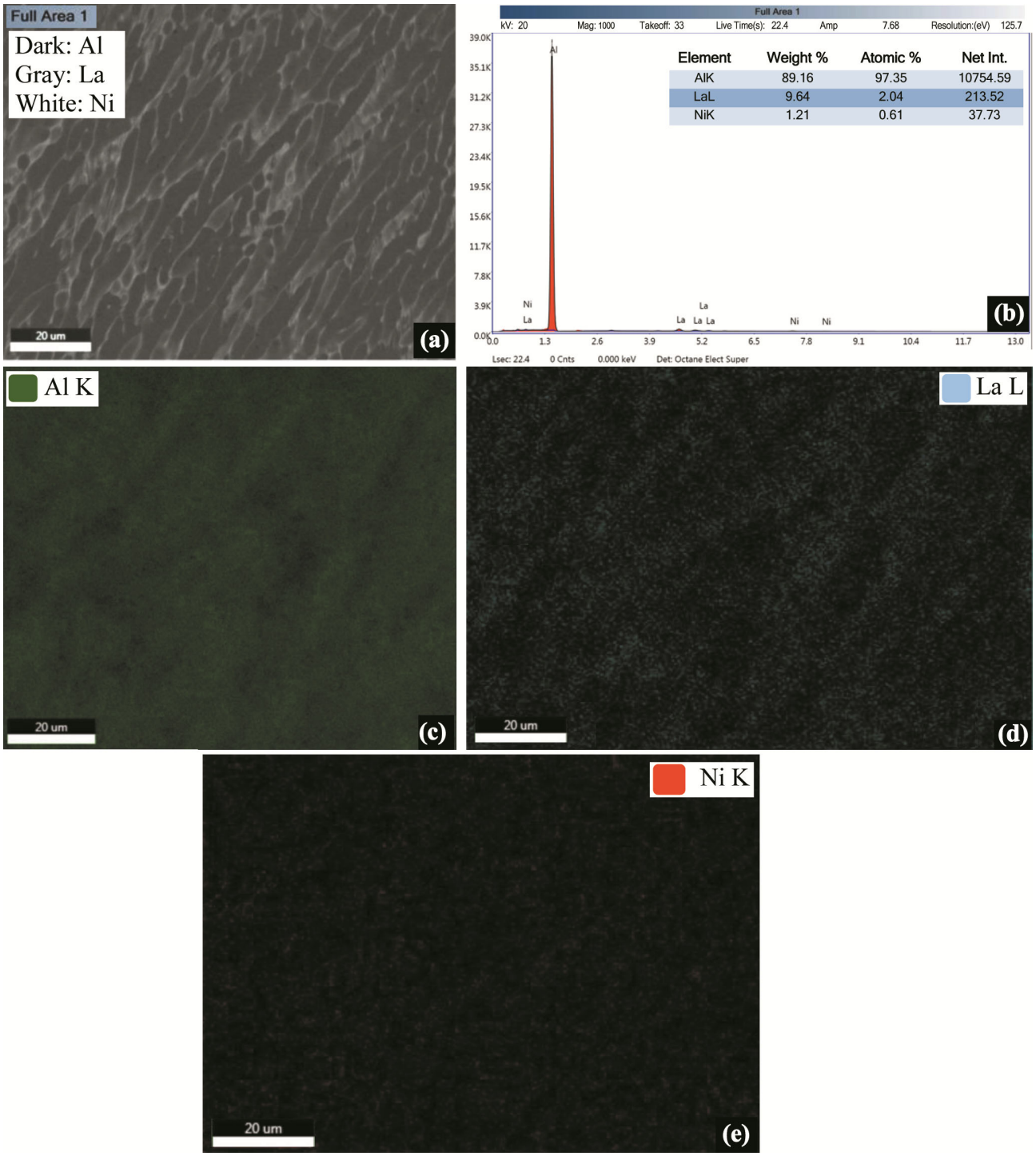

Fig. 3 — Elemental mapping images showing the distribution of chemical elements in the Al-8.8La-1.2Ni cast sample, (a) microstructure of the cast sample, (b) elemental spectrum, and (c, d, e) distributions of Al, La and Ni elements, respectively.

flow technique for this alloy, they reported that the λ values decreased from 182 to 144 W/m K as the T increased from 373 K to 823 K. Murthy *et al.* [25] produced Al-3.25 Zn-1.9 Mg-1.8 Cu alloy with stir casting technique and then applied hot forging to this alloy. They reported that λ values reduced from 127 to 122 W/m K in the range of temperature 323-523 K. In another study, Huang *et al.*[33] calculated the λ values of Al-1Mg alloy by CALPHAD method. They reported that λ values decreased from 208 to 195 W/m K in the range of temperature 600-900 K.

The λ values obtained by us a wider temperature range were lower than the λ values obtained by Smith[35] and Huang *et al.*[33] for various Al-based alloys, but it is slightly higher than the values obtained by Murthy *et al.*[25] and Çadırlı *et al.*[37].

As can be understood from these present results, not only T has an effect on λ, but also minor additions

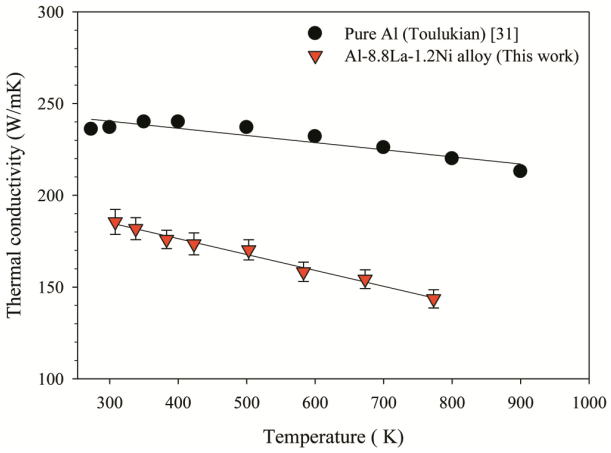

Fig. 4 — The change of λ versus T for Al-8.8La-1.2Ni alloy, and pure Al.

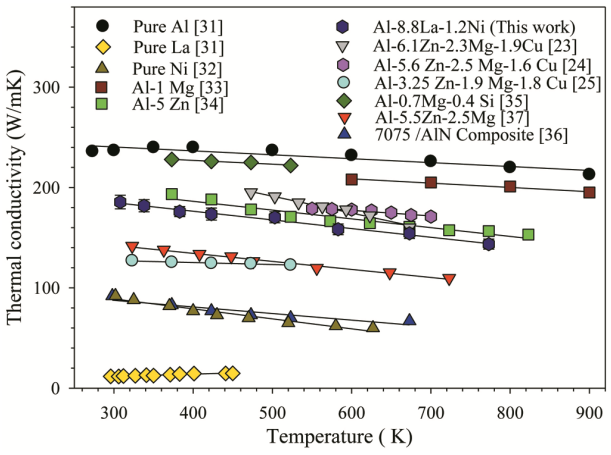

Fig. 5 — The variations of λ versus T for the pure Al, La, Ni, Al-8.8La-1.2Ni alloy, and other Al-based alloys.

of elements, heat treatment and mechanical processing are highly effective.

The α_{TTC} values of pure metals and studied alloy were calculated from Eq. 3(b) with the λ-T curves seen in Fig. 5. As shown in Table 2, the α_{TTC} values for the pure Al, pure La, pure Ni and studied alloy were calculated as -2.25×10^{-4}, 17.2×10^{-4},-10.7×10^{-4}, and -4.86×10^{-4} K^{-1} in the 308-773 K temperature range, respectively.

The major factors that affect the λ values of the alloy were the presence of intermetallic compounds (IMCs), the grain size and the solute atoms in the matrix. In common, the solute atoms dissolved in the matrix can decrease the λ values of the alloys. In a previously study [30] of the authors, α-Al, $Al_{11}La_3$ and Al_3Ni IMCs were observed in XRD analysis for the studied alloy. If the diffusion in the solid was not neglected during the experimental process, both the dissolved atoms and the IMC phase number increased with the increase in T and played an important role in the decrease of the λ values of the alloy studied.

3.3 Determination of ΔH, Cp and α

The thermal properties of Al-8.8La-1.2 Ni alloy such as Tm, ΔH and Cp were determined from the heat flow-T curve obtained using the DSC analysis technique. The variation of the heat flow with T for studied alloy sample is given in Fig. 6. This DSC curve shows the main transition point (T_{peak}) at around 939.2 K. This peak (sharp peak) has been occurred during the completely melting process. For the alloy studied, melting started at 914.7 K (T_{onset}) and melting completely occurred at 939.2 K (T_{peak}). As a result of the calculations with the help of this curve, ΔH and C_p were determined as 280.9 J/g and 0.422 J/g K during the solid-liquid transformation, respectively.

Figure 7 shows the T dependence of Cp for the pureAl[38], studied alloy and other Al-based alloys[24, 35, 37, 39-41]. As shown in this figure, the Cp values of these materials increased with increasing T.

In Table 3, the empirical relationships[42, 43] used in the calculation of the Cp for liquid and solid phases of

Table 2 — Determined values of the α_{TTC} of the pure Al, La, Ni and studied alloy in the different range of temperature

Material	$\alpha_{TTC}x(10^{-4})$ (K^{-1})	T range (K)
Pure Al	-2.25 [31]	273-900
Pure La	17.2 [31]	296-450
Pure Ni	-10.7 [32]	302-627
Al-8.8La-1.2Ni	-4.86 (This work)	308-773

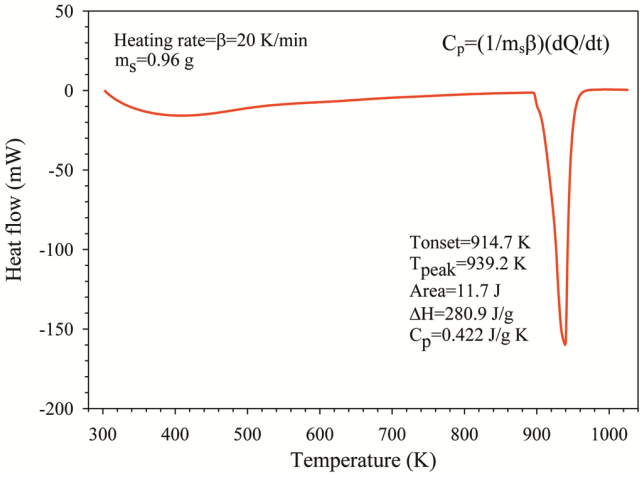

Fig. 6 — Variation of heat flow versus temperature for Al-8.8 La-1.2Ni alloy.

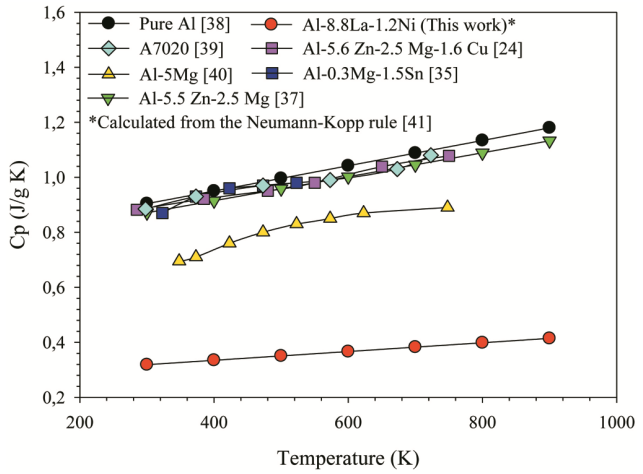

Fig. 7 — The variations of Cp versus T for the pure Al, Al-8.8La-1.2Ni alloy, and other Al-based alloys.

Table 3 — Specific heat of the pure Al, La and Ni metals

Material	Cp (liquid) (J/g K)	Cp (solid) (J/g K)
Pure Al	1.18 [42]	$4.94+2.96\times10^{-3}$ T [42]
Pure Ni	0.63 [43]	$7.80-0.47\times10^{-3}$ T-$1.33\times10^{-5}T^{-2}$ [43]
Pure La	0.19 [42]	$6.65-0.52\times10^{-3}T-0.45\times10^{-5}T^{-2}$ [42]

pure Al, Ni and La are shown. Change of Cp versus T for the studied alloy was calculated numerically by Neumann-Kopp Rule (NKR)[41]. As given in Table 3, the Cp values for the liquid phases of the alloy components (Al, La and Ni) are generally constant, but the Cp values increases with the increase in temperature in the solid phases. The values calculated from NKR[41] for the studied alloy were found as 0.32 and 0.41 J/g K for 300 and 900 K, respectively. In other words, there has been approximately 30% increase in the calculated Cp value in the range of 300-900 K. The Cp value (0.41) calculated from NKR[41] for 900 K overlaps with the experimentally determined 0.42 value during solid-liquid transformation.

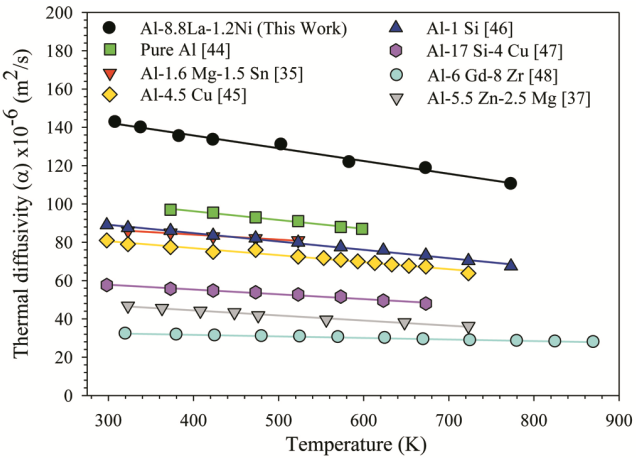

Fig. 8 — The variations of α versus T for the pure Al, Al-8.8La-1.2Ni alloy, and other Al-based alloys.

The values of α were calculated by inserting the λ, ρ, and Cp data in Eq. (5) for studied alloy. As shown in Eq.(6), ρ varies as a function of T. The ρ of studied alloy at RT has been calculated as approximately 3.08 g/cm^3. This situation has been taken into account for the studied alloy. Variations of the α with T for the pure Al[44], the studied alloy and some Al-based alloys [35, 37, 45-48] are shown in Fig. 8.

The values of α of these materials [35, 44-48] decreased with increasing T. For the Al-La-Ni alloy, with the rise of T (from 308 to 773 K), the value of α reduced from 142.78×10^{-6} to 110.51×10^{-6} m^2/s. In addition, there was a decrease of approximately 22.6% in the α value calculated in the range of 308-773 K. As shown in Fig. 8, the values obtained from our study are higher than both pure Al[44] and other Al-based alloys[35, 37, 45-48]. Dilution of alloys may play an important role in the α values for alloys that close to each other in terms of element and content. As seen in Fig. 8, our values (α) being higher than pure Al[44] supports this statement.

4 Conclusion

Thermal properties such as λ, ΔH, Cp and α of the studied alloy were investigated depending on the T. The results are summarized as follows:

- The thermal conductivity values of the studied alloy were measured for different temperatures using the comparative cut bar method. T values

increased from 308 to 773 K, while λ values decreased from 185 to 143 W/m K. There was a decrease of about 23% in the λ value for this temperature range. The α_{TTC} value from the λ-T graph was determined as -4.86×10^{-4} K^{-1}.

- The melting started at 914.7 K and melting completely occurred at 939.2 K for the studied alloy. The value of ΔH and the Cp are 280.9 J/g and 0.422 J/g K, respectively.
- While the Cp values calculated from NKR [41] for the studied alloy increase (from 0.32 to 0.41 J/g K) with increasing T, the α values decreased. The α values (calculated) decreased from 142.78×10^{-6} to 110.51×10^{-6} m^2/s in the range of 308 to 773 K.

References

1 Smallman R E, & Ngan A H W, *Modern physical metallurgy*, 8th. edn, (Butterworth- Heinemann, New York) (2014).
2 Kumar S, & Namboodhiri T K G, *B Mater Sci*, 34 (2011) 311.
3 Rao G S, Rao V V S, & Rao S R K, *Met Sci Heat Treat*, 59 (2017) 139.
4 Cao L, Yang Y, Jiang P, Zhou Q, Mi G, Gao Z, Rong Y, & Wang C, *Results Phys*, 7 (2017) 1329.
5 Assael M J, Dix M, Gialou K, Vozar L, & Wakeham W A, *Int J Thermophys*, 23 (2002) 615.
6 Wang H, Dinwiddie R B, Gustavsson M, & Gustafsson S E, *Therm Cond*, 28 (2006) 199.
7 Manohar K, Yarbrough D, & Booth J, *J Test Eval*, 28 (2000) 345.
8 De Wilde P, Griffiths R, & Goodhew S, *Build Simul*, 1 **(**2008) 36.
9 De Wilde P, Griffiths R, & Goodhew S, *J Build Perform Simul*, 2 **(**2009) 85.
10 Mehling H, Hautzinger G, Nilsson O, Fricke J, Hofmann R, & Hahn O, *Int J Thermophys*, 19 (1998) 941.
11 Le Niliot C, Rigollet F, & Petit D, *Int J Heat Mass Trans*, 43 (2000) 2205.
12 Wang X, Hu H, & Xu X, *J Heat Trans*, 123 (2001) 138.
13 Taketoshi N, Baba T, & Ono A, *Meas Sci Technol*, 12, **(**2001) 2064.
14 Xamán J, Lira L, & Arce J, *Appl Therm Eng*, 29 (2009) 617.
15 Gündüz M, & Hunt J D, *Acta Metall*, 33 (1985) 1651.
16 Corsan J M, *Axial heat flow methods of thermal conductivity measurement for good conducting materials*. In: Maglić K D, Cezairliyan A, Peletsky V.E. (eds) *Compendium of thermophysical property measurement methods*, (Springer, Boston) (1992).
17 ASTM E1225-04, *Standard test method for thermal conductivity of solids by means of the guarded-comparative-longitudinal heat flow technique* (2004).
18 Changhu X, Colby J, Heng B, & Jeffrey P, *Meas Sci Technol* 22 (2011) 075702.
19 Baek Y, Yonghwan R, & Yong K, *Mat Sci Eng C* 26 (2006) 805.
20 Sweet J N, Roth E P, Moss M, Haseman G M, & Anaya J A (Report No SAND 86-0840, Sandia National Laboratories, 1986).
21 Pillai C G S, & George A M, *Int J Thermophys*, 12 (1991) 563.
22 Didion D, (Report No AD665789*,* Springfield, VA: National Technical Information Service, 1968).
23 Li X, & Yu J J, *J Mater Eng Perform* 22 (2013) 2970.
24 Hamilton C, Sommers A, & Dymek S, *Int J Mach Tool Manu*, 49 (2009) 230.
25 Murthy K V S, Girisha D P, Keshavamurthy R, Varol T, & Koppad P G, *Prog Nat Sci-Mater* 27 (2017) 474.
26 Pariona M M, Rugenski J K, Canté M V, Spinelli J E, & Garcia A, *Finite Elem Anal Des*, 46 (2010) 889.
27 Bayram Ü, & Maraşlı N, *J Alloy Compd*, 753 (2018) 695.
28 Inoue A, Kohinata M, Tsai A, & Masumoto T, *Mater Trans JIM* 30 (1989) 378.
29 Dantzer P, *J Less-Common Met*, 131 (1987) 349.
30 Üstün E, & Çadırlı E, *J Alloy Compd*, (2020) 157331.
31 Touloukian Y S, Powell R W, Ho C Y, & Klemens P G, *Thermal conductivity metallic elements and alloys*, (New York, Plenum) (1970).
32 Wen S, Liu Y, Kaptay G, & Du Y, *J Mater Sci Technol*, 59 (2020) 72.
33 Huang L, Liu S, Du Y, & Zhang C, Calphad, 62 (2018) 99.
34 Erol H, Çadırlı E, Erol E A, & Gündüz M, *Int J Cast Metal Res*, 32 (2019) 95.
35 Smith L, *The development and processing of novel aluminum powder metallurgy alloys for heat sink applications*, Master's thesis, (Dalhousie University, Halifax, Nova Scotia, 2013).
36 Kalemtaş A, Topateş G, Bahadır O, İşçi P K, & Mandal H, *T Nonferr Metal Soc*, 23 (2013) 1304.
37 Çadırlı E, Üstün E, Büyük U, & Kaya H, *Kovove Mater*, 59 (2021) 59.
38 Brandes E A, *Smithells metals reference book*, 5th Edition, (Butterworth, London&Boston) (1976).
39 Muhsin J J, Moneer H T, & Muhammed A M, *J Eng Appl Sci*, 7 (2012) 436.
40 Wei G, Huang P, Xu C, Liu D, Ju X, Du X, Xing L, & Yang Y, *Sol Energy*, 137 (2016) 66.
41 Gopal E S R, *Specific heats at low temperatures*, (Plenum Press, New York) (1966).
42 Mills K C, *Recommended values of thermophysical properties for selected commercial alloys*, National Physical Laboratory and ASM International, (Woodhead Publishing Limited, Cambridge) (2002).
43 Smithells C J, *General physical properties*, metals reference book, 7th Edition, Brandes E A & Brook G B, Ed., (Butterworth-Heinemann, New York) (1992).
44 Touloukian, Y S, Powell R W, Ho C Y, & Nicolaou M C, *Thermophysical properties of matter*, vol. 10, *Thermal diffusivity*: Eds. Touloukian Y S, & Ho C Y, (IFI/Plenum, New York) (1973).
45 Choi S W, Cho H S, & Kumai S, *J Alloy Compd*, 688 (2016) 897.
46 Kim Y M, Choi S W, & Hong S K, *J Alloy Compd*, 687 (2016) 54.
47 Zhang C, Du Y, Liu S, Liu S, Jie W, & Sundman B, *Int J Thermophys*, 36 (2015) 2869.
48 Bykov V, Uporov S, & Kulikova T, *T Nonferr Metal Soc*, 25 (2015)1911.